Molecular Crystals and Liquid Crystals

ISSN: 1542-1406 (Print) 1563-5287 (Online) Journal homepage: http://www.tandfonline.com/loi/gmcl20

Substance-P Immobilized Chitosan Nanofibers

Min Sup Kim, Sang Jun Park, Bon Kang Gu, Chang-Mo Kang & Chun-Ho Kim

To cite this article: Min Sup Kim, Sang Jun Park, Bon Kang Gu, Chang-Mo Kang & Chun-Ho Kim (2014) Substance-P Immobilized Chitosan Nanofibers, Molecular Crystals and Liquid Crystals, 603:1, 146-156, DOI: 10.1080/15421406.2014.968078

To link to this article: http://dx.doi.org/10.1080/15421406.2014.968078

Mol. Cryst. Liq. Cryst., Vol. 603: pp. 146–156, 2014

ISSN: 1542-1406 print/1563-5287 online
DOI: 10.1080/15421406.2014.968078

Taylor & Francis
Taylor & Francis Group

Substance-P Immobilized Chitosan Nanofibers

MIN SUP KIM, SANG JUN PARK, BON KANG GU, CHANG-MO KANG, AND CHUN-HO KIM*

Laboratory of Tissue Engineering, Korea Institute of Radiological and Medical Sciences, Seoul, Korea

The surface of biodegradable chitosan nanofibers was functionalized with pristine amine groups and used for immobilization of substance-P, which mediates pain perception and regulates wound healing, inflammation, and angiogenesis. The objectives of this study were to develop substance-P immobilized chitosan nanofibers and to evaluate the biological effects of the immobilized substance-P. Under the same conditions, the amount of substance-P covalently immobilized on chitosan nanofibers was 72.5 ± 16.9 ng compared to 7.3 ± 2.2 ng in passively absorbed samples. Substance-P on chitosan nanofibers released slowly and promoted greater proliferation (∼1.4-fold) of human mesenchymal stem cells than pristine samples after 7 days in culture.

Keywords Chitosan; substance-P; wound healing; electrospinning; human mesenchymal stem cell; tissue engineering

1. Introduction

Electrospinning is a technique that produces nanoscale-diameter polymer fibers. This is accomplished by applying a high voltage to a polymer solution ejected from a needle, causing the solution to extend toward a grounded collector. As the polymer jet travels to the grounded collector, the solvent evaporates and solid polymer fibers are deposited on the collector [1]. Electrospun nanofibers are of interest in biomedical research because they may closely mimic the nanofibrous structure of the native extracellular matrix [2–4]. As a cell culture substrate, nanofibers produced by electrospinning offer a high surface-area-to-volume ratio, which would allow for increased cellular interactions with the material. A variety of biomaterials, including synthetic and natural polymers, have been examined as electrospinning substrates for tissue engineering applications [5]. Natural polymers have attracted attention in tissue engineering owing to their beneficial properties, such as hydrophilicity, low immunogenicity, non-toxicity, and similarity to the extracellular matrix [6–8]. One such natural polymer is chitosan, derived from sea crustaceans. Chitosan is partially or completely deacetylated chitin and is composed of glucosamine and N-acetyl-glucosamine in a β (1–4) linkage. Chitosan is good candidate material for tissue engineering applications because it is non-immunogenic, biocompatible, biodegradable, and possesses desirable hemostatic properties [9–11]. Also, because chitosan contains amino groups, it is polycationic, which ultimately gives rise to unique functional properties [12–15]. Therefore, electrospun nanofibers based on natural polymers could present a high

*Address correspondence to Chun-Ho Kim, Laboratory of Tissue Engineering, Korea Institute of Radiological and Medical Science, Seoul Korea. E-mail: chkim@kcch.re.kr

surface area onto which various bioactive molecules, such as enzymes, antibodies, growth factors and synthetic peptides, could be immobilized at high density for tissue engineering applications [16–19].

Substance-P (SP), a pro-inflammatory neuropeptide released from sensory nerves, modulates wound healing, migration and proliferation of inflammatory cells, and angiogenesis [20–23]. In its capacity as an active wound-healing agent, SP induces the mobilization and migration of mesenchymal stem cells (MSCs) from bone marrow [24, 25]. However, SP is generally unstable, and soluble bioactive factors are rapidly excreted from the injected site and are often enzymatically digested or deactivated [26, 27]. Thus, developing a delivery system that allows desired functions to be retained is a key to the success of therapeutic applications of bioactive proteins. In this context, Koharaet al. reported achieving the controlled release of SP using hydrogels prepared from an anionic gelatin derivative, resulting in enhanced granulocyte recruitment and angiogenesis induction [28]. Because of their high surface-to-volume ratio, chitosan nanofibers (CNs) provide definite advantages as SP delivery vehicles for implantable devices or wound dressing materials.

In this study, we fabricated CNs by electrospinning and then sequentially immobilized SP on CNs using a peptide-coupling agent. We then examined the effects of SP concentration on nanofibers morphology and the releasing behavior of immobilized SP. To explore possible tissue engineering applications, we also investigated the effect of SP content on metabolic activity by culturing human MSCs (hMSCs) on SP-immobilized CNs.

2. Materials and Methods

2.1. Materials

Chitosan (average molecular weight: 370 kDa; deacetylation degree: 75%), trifluoroacetic acid (TFA), dichloromethane (MC), and 4-morpholine ethane sulfonic acid sodium salt (MES) were purchased from Sigma-Aldrich (St. Louis, MO, USA). Acetic acid (extra pure grade) was purchased from Junsei Chemical Industries (Chuo-ku, Osaka, Japan). Ethanol and methanol (absolute for analysis) were purchased from Merck (Darmstadt, Germy). Paraformaldehyde, Triton X-100, dimethyl sulfoxide, and sodium hydroxide (NaOH) were purchased from Sigma-Aldrich. Albumin Fraction V (from bovine blood, BSA) was purchased from Amersham/USB (Arlington Heights, IL, USA). SP (molecular weight: 1347.6 Da) was purchased from Calbiochem (Frankfurter, Darmstadt, Germany). Low-glucose Dulbecco's modified Eagle's medium (DMEM), Dulbecco's phosphate-buffered saline (DPBS), and 0.05% trypsin-EDTA were purchased from Gibco BRL (Carlsbad, CA, USA). Fetal bovine serum (FBS) and penicillin-streptomycin (p/s) were purchased from WelGene Inc. (Daegu, South Korea). Cell Counting Kit-8 (CCK-8) was purchased from Dojindo Laboratories (Kumamoto, Japan).

2.2. Preparation of Chitosan Nanofibers

Following a conventional electrospinning procedure, a 5% (w/v) chitosan solution (dissolved in TFA:MC at a 7:3 volume ratio) was injected from a stainless steel needle connected to a syringe using a syringe pump (KD Scientific, Holliston, MA, USA) at a rate of 1 ml/h. A voltage of 18 kV was applied between the syringe needle and the grounded collector using a high-voltage power supply (Wookyung Tech, Incheon, Korea); the collector was placed 15 cm below the tip of the needle to collect the nanofibers. The resulting

nanofibers were dried overnight at room temperature and then neutralized to eliminate acidic salt residues by immersion in 3M NaOH (dissolved in methanol) for 30 minutes [29]. The neutralized CNs were then rinsed sequentially with 70% and 50% methanol and deionized water. Finally, nanofibers were lyophilized at −80°C in a vacuum (5 mTorr) for 1 day.

2.3. Immobilization of SP on Chitosan Nanofibers

CNs were functionalized with SP using a covalent immobilization technique [16, 30, 31]. In brief, the nanofibers were soaked in 10 ml of 0.1M MES buffer (pH 6.7) containing 0.1 mM of N-hydroxysuccinimide (NHS) with gentle agitation for 2 hours at room temperature. After washing five times with MES buffer, the activated nanofibers were soaked in MES buffer containing different concentrations of SP (0, 25, 50, and 100 ng per mg of nanofibers) and then were shaken for 12 hours at 4°C to yield SP-conjugated carbon nanofibers (SP-CNs). For comparison with SP immobilization, 100 ng SP was passively absorbed onto CNs (PA SP-CNs). Finally, the resulting samples were washed with DPBS and lyophilized.

2.4. Morphological Characterization

The morphology of CNs was investigated using a MIRA II field emission-scanning electron microscope (FE-SEM; Tescan, Libusinatr 21, Czech Republic). Samples were mounted onto stubs and coated with gold using a sputter coater (Eiko IB3; Tokyo, Japan). The average diameter of nanofibers was measured by selecting 10 fields from each image and manually measuring fiber diameters using a ruler generated within the image analyzer (Image Pro-Plus; Media Cybernetics, Inc., MD, USA).

2.5. Analysis of SP Immobilized on Nanofibers

Immobilized SP on CNs was quantified using an enzyme-linked immune sorbent assay (ELISA) kit (R & D Systems, McKinley, MN, USA). A 50 μl solution containing SP that had remained in solution after the immobilization of SP was mixed with 50 μl of standard diluent buffer, and then incubated in an ELISA plate for 2 hours at room temperature. After rinsing four times, 100 μl of biotin conjugate was added and plates were incubated for 1 hour. The plates were then rinsed and sequentially incubated with 100 μl of streptavidin and stabilized chromogen, and added to the wells of the ELISA plate. After addition of stop solution, the optical density (OD) of the solutions was read at 450 nm using a plate reader. SP concentrations in the solution were determined by reference to a standard calibration curve prepared using known concentrations of SP.

SP immobilization was confirmed by first labeling SP with the fluorescent probe, fluorescein isothiocyanate (FITC), using a Fluoro Tag FITC conjugation kit (Sigma- Aldrich), following the manufacturer's protocol. FITC-labeled SP was then immobilized on CN, as described above. After the immobilization process, the samples were embedded in optimal cutting temperature (OCT) compound (Tissue-Tek, Torrance, CA, USA), frozen and cut into 10-μm-thick sections at −28°C; sections were visualized using confocal laser-scanning microscopy (EZ-C1; Nikon Corp., Chiyoda-ku, Japan).

2.6. Kinetics of SP Release from Nanofibers

The kinetics of SP release from CNs was determined by incubating the samples in 5 ml of DPBS at 37°C with continuous agitation. Over the course of one week incubation, 100 μl samples were collected at 0.5, 1, 3, 5, and 7 days. The cumulative amount of released SP in the collected solution was determined using an ELISA kit, as described above.

2.7. Viability of hMSCs on SP-Immobilized Nanofibers

hMSCs (Lonza,Basel, Switzerland) were maintained in DMEM supplemented with 10% FBS and 1% p/s under standard culture conditions (37°C, 5% CO_2). When cells had reached approximately 70% confluence, they were enzymatically detached and seeded onto the nanofibers at a density of 2×10^3 cells/cm^2 (passage number 7) in DMEM containing 10% FBS and 1% p/s. After 1 day of culture, the medium was changed to DMEM containing1% FBS and 1% p/s. The viability of hMSCs grown on CNs was evaluated at designated time points (1, 4, and 7 days) using CCK-8 assays, as described by the manufacturer. Briefly, cell-seeded samples (n = 4) were rinsed with DPBS, and 500 μl CCK solution was added to the samples. After 3 hours, absorbance of the solution at 450 nm was measured using a plate reader.

At 1, 4 and 7 days post-seeding, hMSCs cultured on nanofibers were immunostained using Alexa Fluor 488 phalloidin (Invitrogen) and counterstained with 4′, 6-diamidino-2-phenylinodole (DAPI, Invitrogen) to label actin filaments and nuclei, respectively. Cells on nanofibers were investigated using confocal laser-scanning microscopy.

2.8. Statistical Analysis

Quantitative data were obtained in triplicate and are reported as means ±standard deviations, where indicated. Statistical analyses were performed using a one-way analysis of variation (ANOVA), followed by Tukey's HSD test for multiple comparisons. A p-value < 0.05 was considered statistically significant.

3. Results and Discussion

First, we investigated the morphological stability of CNs prepared via the aqueous, covalent-immobilization process. SEM images of pristine (non-neutralized) CNs (Fig. 1A) revealed randomly oriented nanofibers that formed three-dimensional open pores that were homogeneously distributed throughout the structure. In contrast, nanofibers of CNs neutralized with NaOH maintained a uniform, interconnected nanofibrous structure (Fig. 1B), consistent with our previous study using an NaOH neutralization process [29]. Moreover, this nanofibrous structure of CNs was maintained during the SP-incorporated process (Fig. 1C and 1D). Collectively, these observations indicate that neutralization and covalent immobilization had a minimal effect on the overall morphology of each fiber.

However, after completing these steps, the fibers did make closer contact with the underlying fibers and showed a deformed structure, particularly at fiber-fiber junctions (compare to Fig. 1A). To quantitatively analyze these subtler morphological changes, we measured the average fiber diameters of nanofibers from SEM images. As shown in Fig. 2, the average fiber diameter of pristine CN was 218.41 ± 22.51 nm and increased to 339.25 ± 27.67 nm after the neutralization process. A possible explanation for this phenomenon is that incorporation of a small amount of water resulted in the partial hydrolysis or dissolution

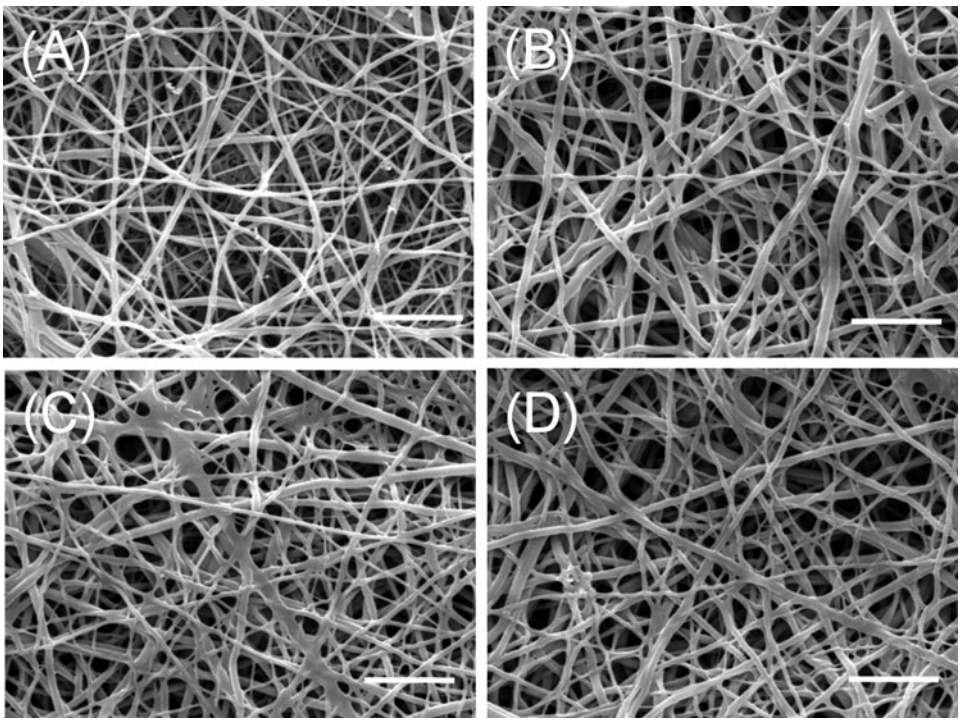

Figure 1. (A) Representative SEM images of (A) pristine and (B) neutralized chitosan nanofibers (CN), (C) passively absorbed SP on nanofibers, and (D) covalently SP immobilized nanofibers, respectively. Scale bar is 5 μm.

of the chitosan component during the neutralization process [32]. Average fiber diameters of passively absorbed PA SP-CN samples (336.72 $\pm$ 21.29 nm) and covalently immobilized (SP-CN) samples (331.82 $\pm$ 19.51 nm) were not significantly different from those of neutralized chitosan samples.

The amount of SP immobilized on nanofibers was quantified by ELISA. As shown in Fig. 3, the amount of SP passively immobilized on CN in a solution containing 100 ng SP per milligram CN was 7.34 $\pm$ 2.15 ng. In contrast, the amount of SP on CNs following covalent immobilization at the same SP concentration was approximately 10-fold higher (72.5 $\pm$ 16.9 ng). The amount of SP covalently immobilized on nanofibers was highly dependent on the initial concentration of SP. At 25 and 50 ng SP/mg nanofibers, the amount of SP immobilized was 15.97 $\pm$ 8.29 and 33.21 $\pm$ 11.42 ng, respectively. The amount of SP immobilized was similar at SP concentrations greater than 100 ng/mg CN (e.g., 78.42 $\pm$ 19.61 vs. 72.5 $\pm$ 16.9 ng at 200 and 100 ng SP/mg CN, respectively), indicating that the immobilization reaction saturates in this concentration range.

Fluorescence images confirmed that SP immobilization was not affected by the thicknesses (approximately 100 μm) of the nanofibers, as shown in Fig. 4. FITC-conjugated SP could be observed throughout cross-sectional areas of entire samples, owing to the porous nature of the nanofibers.

The release kinetics of SP from the nanofibers are shown in Fig. 5. PA SP-CN samples showed an initial burst of release, resulting in the release of 82.0 $\pm$ 10.6% and 93.7 $\pm$ 4.9% of SP within 0.5 and 1 day, respectively; no further release was observed thereafter. However,

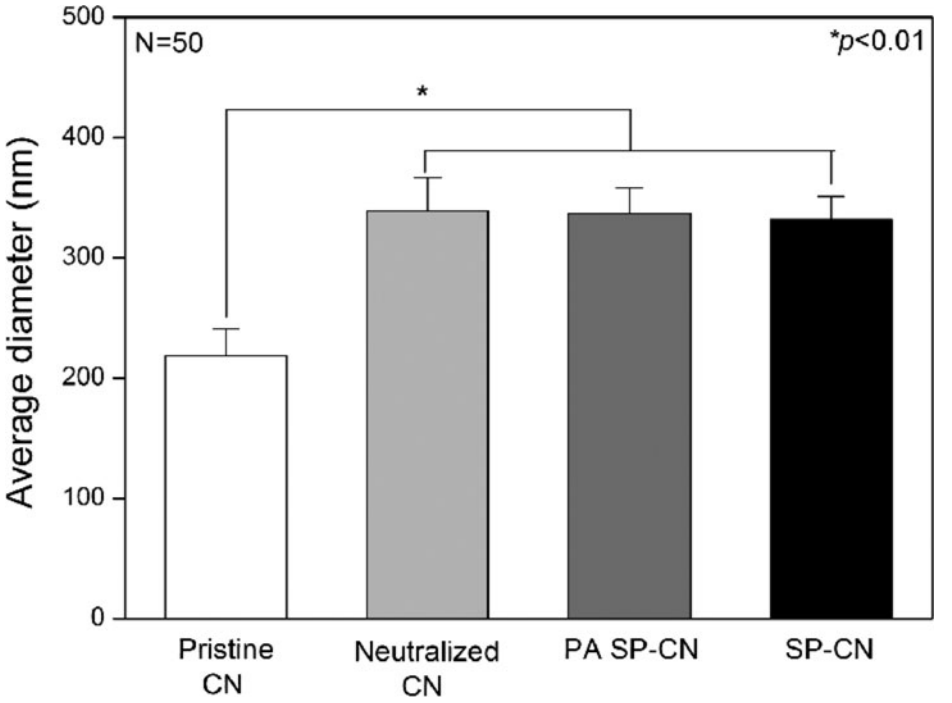

Figure 2. Average fiber diameters of CN. To measure the average diameter of nanofibers, 10 fields from each image were selected and the fiber diameters were manually measured.

SP-CN samples showed minimal release of SP over the course of 7 days. For example, SP-CNs immobilized at starting SP concentrations of 25, 50, and 100 ng/mg released 2.7 ± 1.7%, 2.5 ± 1.5%, and 2.4 ± 0.8% after 1day, respectively; the corresponding values for SP release after 7 days were 11.0 ± 1.2%, 10.3 ± 1.2%, and 11.5 ± 1.3%. The release of immobilized SP from nanofibers appeared to be linear and limited regardless of the amount of immobilized SP. Collectively, these results indicate that covalent bonding of SP on nanofibers controlled the release of SP *in vitro*, and therefore would be predicted to provide long-term protection against the degradation of SP *in vivo*. Consistent with this latter supposition, Kim et al. showed that SP, covalently immobilized in self-assembling peptides, was released over 28 days, and subsequently efficiently promoted migration and proliferation of MSCs in a mouse ischemia model [25].

The adhesion and proliferation of hMSCs on nanofibers was investigated using the CCK-8 system, a colorimetric assay that reports viability in terms of OD values. As shown in Fig. 6, OD values for hMSCs treated with neutralized CNs (0.34 ± 0.07), PA SP-CNs (0.29 ± 0.09), or SP-CNs (0.31 ± 0.11) were not significantly different on day 1, indicating that viability was not different among groups at this time point. However, on day 4, the OD value of the PA SP-CN group increased significantly to 0.58 ± 0.08, compared to the slight increase of neutralized (0.41 ± 0.04) and SP-CN (0.45 ± 0.12) groups. This higher proliferation of hMSCs in the passively SP-adsorbed group relative to the other groups could be due to the burst release of passively absorbed SP on the first day. On day 7, the OD value of SP-CN samples (0.88 ± 0.06) was greater than that for neutralized (62 ± 0.05) and PA SP-CN (0.67 ± 0.09) samples. This greater proliferation of hMSCs cultured on SP-CNs

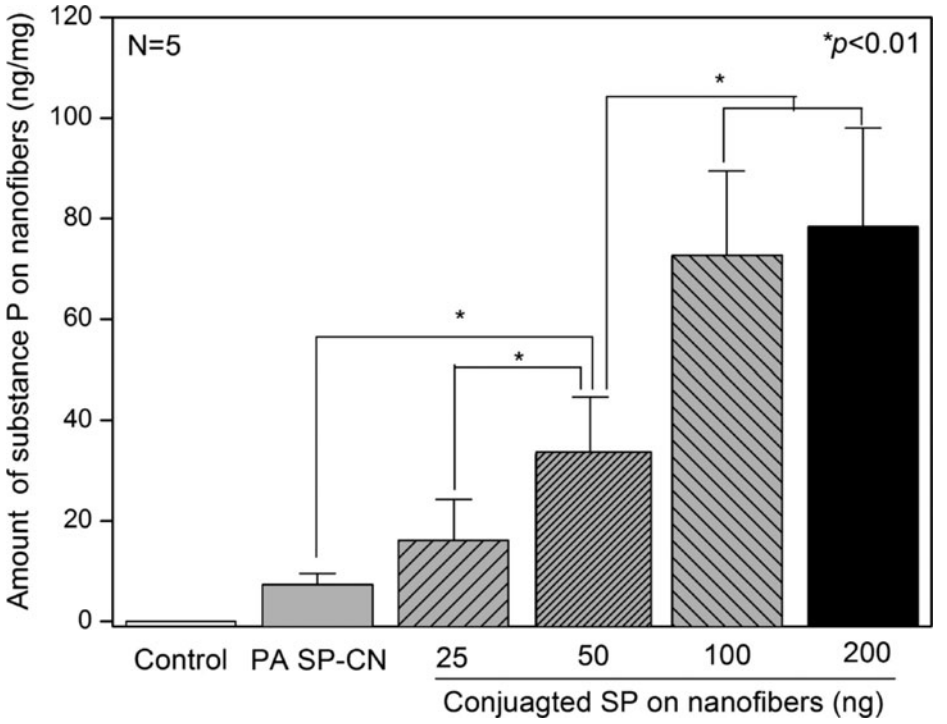

Figure 3. The amount of SP on the nanofibers indirectly was analyzed by using ELISA method. SP (100 ng) was passively adsorbed on the nanofibers (PA SP-CN) and actively immobilized on the nanofibers prepared by reactions with 25, 50, 100, and 200 mg SP.

through day 7 in culture suggests that minimal release and locally high concentrations of SP induce higher levels of metabolic activity in hMSCs. These results confirm that, despite being physically adsorbed or covalently bound, SP promotes the metabolic activities of MSCs, as reported by Hong HS et al. [24, 33].

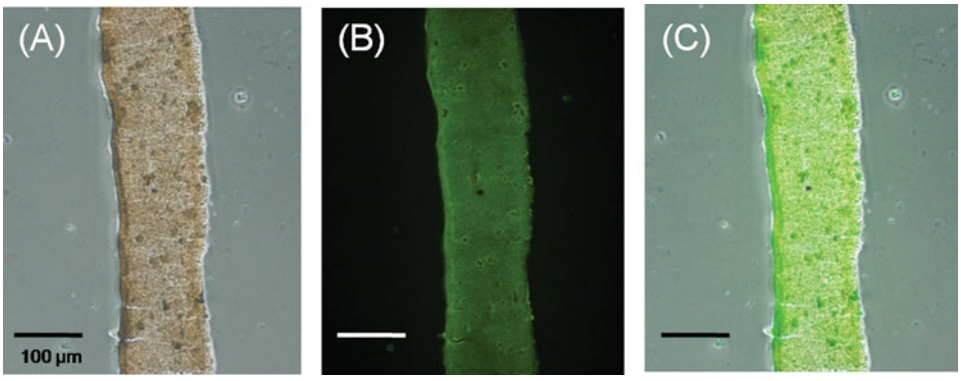

Figure 4. CLSM images of FITC labeled SP (FITC-SP) on nanofibers. (A) phase contrast, (B) fluorescence, and (C) merged images. The FITC-SP was observed in throughout cross-sectional area of nanofibers. Scale bear is 100 μm.

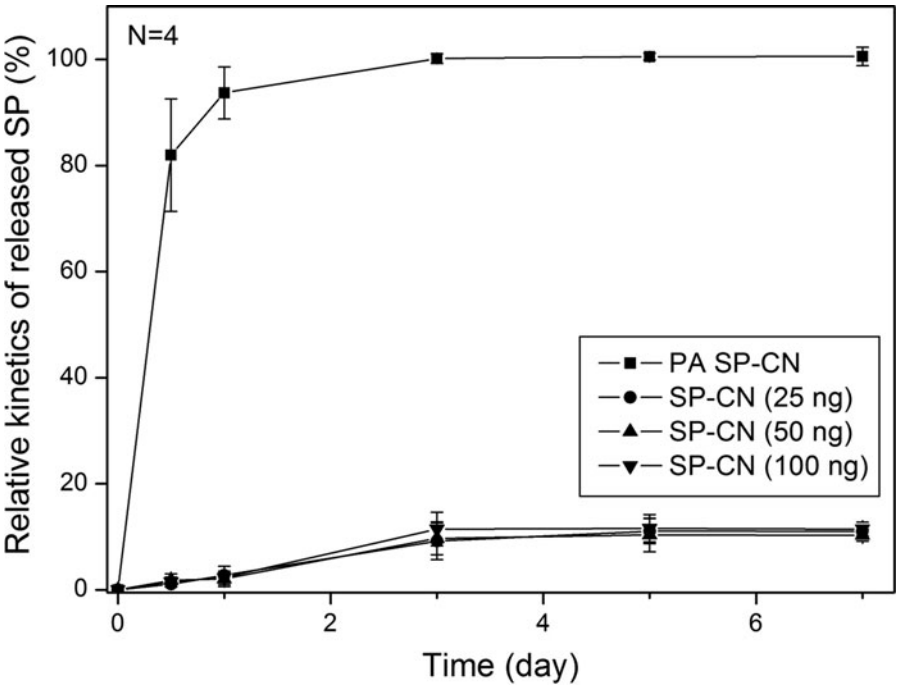

Figure 5. Cumulative release kinetics of SP from the nanofibers at 37° for 7 days.

We confirmed the effects of culturing hMSCs on SP-immobilized nanofibers using immune-fluorescence staining of cell nuclei (blue) and actin filaments (green).As shown in Fig. 7, on day 1 of culture, hMSCs cultured on CNs exhibited a round, thin, spindle-shaped morphology that showed no clear dependence on the presence of SP. On day 4 of culture,

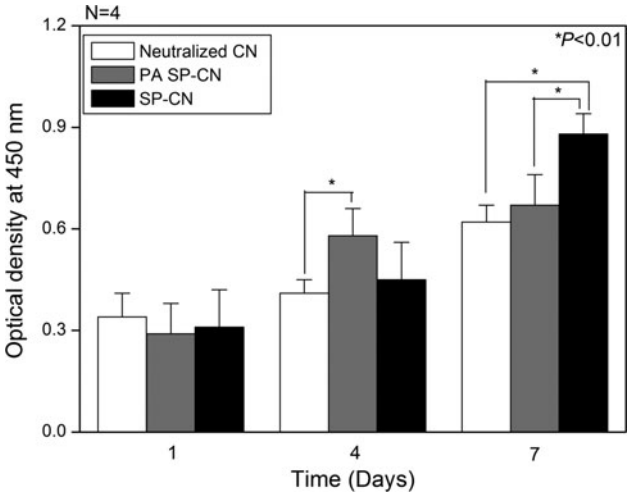

Figure 6. The metabolic activity of human mesenchymal stem cells (hMSCs) on neutralized, PA SP-, and SP-CN in the conditioned media during 7 days.

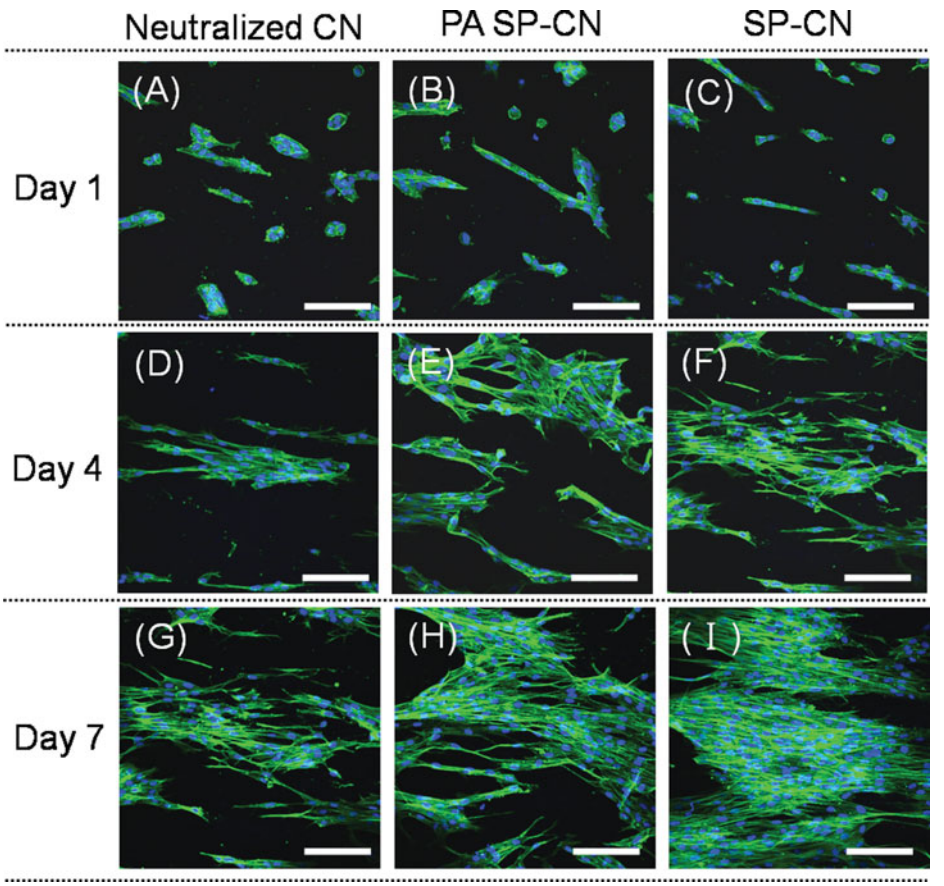

Figure 7. CLSM images of hMSCs on neutralized, PA SP-, and SP-CN after 7 days of cultivation (Scale bear is 100 μm). CLSM images of hMSCs on (A) neutralized CN, (B) PA SP-, and (C) SP-CN on day 1, respectively. And hMSCs on (D) neutralized CN, (E) PA SP-, and (F) SP-CN on day 4, respectively. Finally, hMSCs on (G) neutralized CN, (H) PA SP-, and (I) SP-CN on day 7, respectively. Cell nuclei (blue) and actin filaments (green) were stained by DAPI and Alexa Fluor 488 phalloidin. Scale bar is 100 μm.

the density of hMSCs cultured on PA SP-CN samples was higher than that observed in other groups (Fig. 7E). These results correlate with the initial rapid release of SP from PA SP-CN samples. On day 7 of culture, hMSCs cultured on SP–CNs exhibited much higher density than cells in other groups, with formation of mature actin filaments (Fig. 7I). By contrast, hMSCs cultured on neutralized CN nanofibers showed a thinner, spindle-shaped morphology compared with hMSCs in both SP-CN and PA SP-CN groups (Fig. 7D and 7G). These cellular morphologies were correlated with the metabolic activity of hMSCs, as reflected in the results of CCK-8 assays (Fig. 6).

This study confirmed that SP incorporated nanofibers more effectively promoted metabolic activity of hMSCs *in vitro* compared with nanofibers without SP. Notably, covalently immobilized, bioactive SP was released slowly, greatly enhancing the biological activity of hMSCs. The results obtained using our immobilized SP system could be extended to other bioactive peptides and tissue injuries for use in various MSC therapy applications.

5. Conclusion

In this study, SP immobilized nanofibers were successively fabricated using a peptide-coupling agent. The SP-immobilized nanofibers exhibited morphological stability as a substrate for culturing hMSCs and were capable of controlling the amount and timing of SP release. Moreover, our *in vitro* study revealed that SP incorporated nanofibers were more effective in promoting the cellular metabolic activity of hMSCs. Collectively, our findings suggest that SP incorporated nanofibers hold promise as functional substrates, and in combination with therapeutic peptides, have potential as implants for controlling biological functions in regenerative medicine.

Funding

This work was supported by Industrial Strategic Technology Development Program (10035291, Multi-functional medical fiber complex technology) funded by the Ministry of Knowledge Economy (MKE, Korea) and by Nuclear Research Development Program of the Korea Science and Engineering Foundation grant funded by Ministry of Science, ICT, and Future Planning (MSIP, Korea)

References

[1] Li, D., & Xia, Y. (2004). *Adv. Mater.*, *16*, 1151.
[2] Li, W. J., Laurencin, C. T., Caterson, E. J., Tuan, R. S., & Ko, F. K. (2002). *J. Biomed. Mater. Res.*, *60*, 613.
[3] Barnes, C. P., Sell, S. A., Boland, E. D., Simpson, D. G., & Bowlin, G. L. (2007). *Adv. Drug. Deliver. Rev.*, *59*, 1413.
[4] Park, H. N., Lee, J. B., & Kwon, I. K. (2010). *Int. J. Tissue. Regen.*, *1*, 10.
[5] Sill, T. J., & Von Recum, H. A. (2008). *Biomaterials*, *29*, 1989.
[6] Malafaya, P., Silva, G. A., & Reis, R. L. (2007). *Adv. Drug. Deliver. Rev.*, *59*, 207.
[7] Kim, M. S., Jun, I., Shin, Y. M., Jang, W., Kim, S. I., & Shin, H. (2010). *Macromol. Biosci.*, *10*, 91.
[8] Kim, T. H., Ko, J. H., Kim, S. J., & Park, Y. H. (2011). *Int. J. Tissue. Regen.*, *2*, 1.
[9] Shi, C., Zhu, Y., Ran, X., Wang, M., Su, Y., & Cheng, T. (2006). *J. Surg. Res.*, *133*, 185.
[10] Kim, I.-Y., Seo, S.-J., Moon, H.-S., Yoo, M.-K., Park, I.-Y., Kim, B.-C., & Cho, C.-S. (2008). *Biotechnol. Adv.*, *26*, 1.
[11] Park, S. J., Kim, M. S., Yu, S. M., Gu, B. K., Kim, J.-I., & Kim, C.-H. (2012). *Macromol. Res.*, *20*, 397.
[12] Madihally, S. V., & Matthew, H. W. (1999). *Biomaterials*, *20*, 1133.
[13] Khor, E., & Lim, L. Y. (2003). *Biomaterials*, *24*, 2339.
[14] Laurencin, C. T., Jiang, T., Kumbar, S. G., & Nair, L. S. (2008). *Curr. Top. Med. Chem.*, *8*, 354.
[15] Kim, M. S., Park, S. J., Gu, B. K., & Kim, C.-H. (2012). *Carbohyd. Polym.*, *87*, 2683.
[16] Ho, M.-H., Wang, D.-M., Hsieh, H.-J., Liu, H.-C., Hsien, T.-Y., Lai, J.-Y., & Hou, L.-T. (2005). *Biomaterials*, *26*, 3197.
[17] Ma, P. X. (2008). *Adv. Drug. Deliver. Rev.*, *60*, 184.
[18] Yoo, H. S., Kim, T. G., & Park, T. G. (2009). *Adv. Drug. Deliver. Rev.*, *61*, 1033.
[19] Kim, M. S., Bhang, S.-H., Yang, H. S., Rim, N. G., Jun, I., Kim, S. I., Kim, B.-S., & Shin, H. (2010). *Tissue. Eng. Pt. A.*, *16*, 2999.
[20] Ziche, M., Morbidelli, L., Pacini, M., Geppetti, P., Alessandri, G., & Maggi, C. A. (1990). *Microvasc. Res.*, *40*, 264.
[21] Ziche, M., Morbidelli, L., Masini, E., Amerini, S., Granger, H., Maggi, C., Geppetti, P., & Ledda, F. (1994). *J. Clin. Invest.*, *94*, 2036.
[22] Delgado, A. V., Mcmanus, A. T., & Chambers, J. P. (2005). *Exp. Biol. Med.*, *230*, 271.

[23] Felderbauer, P., Bulut, K., Hoeck, K., Deters, S., Schmidt, W. E., & Hoffmann, P. (2007). *Int. J. Colorectal. Dis.*, *22*, 1475.
[24] Hong, H. S., Lee, J., Lee, E., Kwon, Y. S., Lee, E., Ahn, W., Jiang, M. H., Kim, J. C., & Son, Y. (2009). *Nat. Med.*, *15*, 425.
[25] Kim, J. H., Jung, Y., Kim, B.-S., & Kim, S. H. (2012). *Biomaterials*, 1657.
[26] Post, M. J., Laham, R., Sellke, F. W., & Simons, M. (2001). *Cardiovasc. Res.*, *49*, 522.
[27] Gupta, R., Tongers, J., & Losordo, D. W. (2009). *Circ. Res.*, *105*, 724.
[28] Kohara, H., Tajima, S., Yamamoto, M., & Tabata, Y. (2010). *Biomaterials*, *31*, 8617.
[29] Gu, B. K., Park, S. J., Kim, M. S., Kang, C. M., Kim, J.-I., & Kim, C.-H. (2013). *Carbohyd. Polym.*, 65.
[30] Park, K. M., Lee, S. Y., Joung, Y. K., Na, J. S., Lee, M. C., & Park, K. D. (2009). *Acta. Biomater.*, *5*, 1956.
[31] Han, H. D., Mangala, L. S., Lee, J. W., Shahzad, M. M., Kim, H. S., Shen, D., Nam, E. J., Mora, E. M., Stone, R. L., & Lu, C. (2010). *Clin. Cancer. Res.*, *16*, 3910.
[32] Kim, M. S., Park, S. J., Gu, B. K., & Kim, C.-H. (2012). *J. Nanomater.*, *2012*, 10.
[33] Ko, I. K., Ju, Y. M., Chen, T., Atala, A., Yoo, J. J., & Lee, S. J. (2012). *Faseb. J.*, *26*, 158.